

Original Articles

Spatial distribution and stability mechanisms of soil organic carbon in a tropical montane rainforest

Wenjie Liu^{a,e,1}, Yamin Jiang^{a,1}, Qiu Yang^a, Huai Yang^{b,c,*}, Yide Li^c, Zhaolei Li^d, Wei Mao^a, Yiqi Luo^e, Xu Wang^a, Zhenghong Tan^a

^a School of Ecology and Environment, Hainan University, Haikou 570228, China

^b International Centre for Bamboo and Rattan, Beijing 100102, China

^c Jianfengling National Key Field Research Station for Tropical Forest Ecosystem, Research Institute of Tropical Forestry, Chinese Academy of Forestry, Ledong 510520, China

^d National Engineering Laboratory for Efficient Utilization of Soil and Fertilizer Resources, Key Laboratory of Agricultural Environment in Universities of Shandong, College of Resources and Environment, Shandong Agricultural University, Taian 271018, PR China

^e Center for Ecosystem Science and Society, Northern Arizona University, Flagstaff, AZ 86011, USA



ARTICLE INFO

Keywords:

SOC
Old-growth tropical forest
Spatial distribution
Semi-variance analysis
¹³C CPMAS/NMR

ABSTRACT

Estimation of soil organic carbon (SOC) storage and its dynamics in tropical montane forests is crucial for climate change prediction, which calls for further investigation into the spatial variation in SOC and its stability mechanisms. In this study, 60 subplots (20 m × 20 m) were randomly selected within a 60 ha tropical montane rainforest dynamic monitoring plot located in southern China. The physical (HFC and LFC) and chemical fractions of SOC (alkyl C, O-alkyl C, aromatic C and carbonyl C), microbial biomass carbon and other soil properties at depths of 0–10 cm, plant species and root biomass (0–10 cm and 10–20 cm) were investigated. Geostatistical methods, multiple regression trees and redundant analysis were used to reveal that the spatial variations in SOC and its stability mechanisms with the terrain. The results show that the spatial variations in HFC and the ratios of alkyl carbon/O-alkyl carbon had a moderate spatial dependence due to the complex terrain. High SOC and its physical stability fractions (HFC) were distributed along ridgelines, while the chemical stability index of SOC (alkyl C/O-alkyl C) was the highest on hillsides and in valleys. Terrain convexity best explained the spatial variations in SOC and HFC, while total nitrogen and convexity together best explained the spatial variation in the chemical fractions of SOC. Abiotic factors explained more of the variation in SOC and its fractions than biotic factors, while abiotic and biotic factors were covariant. The specific factors controlling the distribution of SOC and its fractions differed with the types of micro-terrain. These results highlight the influence of terrain on the distribution and accumulation of SOC in tropical forest ecosystems. Hence, terrain should be considered a key factor in biogeochemical models.

1. Introduction

Soil organic carbon (SOC) is the largest terrestrial carbon (C) pool and a key component of the global C cycle (Ciais et al., 2013; Tao et al., 2020). Small changes in the global SOC pool can drastically alter the land–atmosphere C balance and its feedbacks to climate change (Luo et al., 2015; Shi et al., 2018). Forests cover 33% of the terrestrial surface area (Yu et al., 2019) and its SOC plays an important role in the global C

cycle (Cox et al., 2000; Cramer et al., 2001; Pan et al., 2011). Understanding the spatial distribution of SOC and its stability is essential for C estimation, which is helpful in designing management schemes that increase C sinks (Gruba and Socha, 2019). However, modeling the spatiotemporal dynamics of SOC is challenging due to its inherent spatial heterogeneity across complex terrain and data limitations caused by the inaccessibility of forests.

SOC is complex and heterogeneous and consists of fractions that vary

Abbreviations: SOC, soil organic carbon; HFC, heavy fraction of SOC; LFC, light fraction of SOC; MBC, microbial biomass carbon; DOC, dissolved organic carbon; TN, total nitrogen; TP, total phosphorus; MRT, multiple regression tree analysis; RDA, Redundant analysis.

* Corresponding author at: International Centre for Bamboo and Rattan, Beijing 100102, China.

E-mail address: yanghuai2008@163.com (H. Yang).

¹ The two authors contributed equally.

<https://doi.org/10.1016/j.ecolind.2021.107965>

Received 8 February 2021; Received in revised form 11 May 2021; Accepted 6 July 2021

Available online 15 July 2021

1470-160X/© 2021 The Authors.

Published by Elsevier Ltd.

This is an open access article under the CC BY-NC-ND license

(<http://creativecommons.org/licenses/by-nc-nd/4.0/>).

in turnover time from hours to millennia (Trumbore, 1997). According to ^{13}C NMR spectra, the chemical fractions of SOC include alkyl C, O-alkyl C, aromatic C and carboxyl C (Baldock et al., 1992). The alkyl C/O-alkyl C ratio reflects the degree of alkylation of SOC, and has also been used as an index of its decomposability or humification (Zhao et al., 2012), and the stability of SOC. Higher ratios of alkyl C/O-alkyl C indicate more stable fractions in the SOC (Wang et al., 2010), which may benefit SOC accumulation and stability. In addition, physical fractionation methods can also separate SOC into labile and recalcitrant fractions through density fractionation (von Lützow et al., 2007). Heavy fraction carbon (HFC) is a more stable and high-density organomineral fraction of SOC (Golchin et al., 1995). The dynamic accumulation and distribution of SOC is the result of stabilization and destabilization processes that are influenced by factors both biotic (amount, chemical composition, and relative allocation of plant inputs), and abiotic (climate, land surface aspect, slope, and convexity, soil temperature and moisture, texture) (Jackson et al., 2017; Merino et al., 2014). Terrain is one of the important contributors to landscape-scale variation in soil nutrient cycling (Dai et al., 2018; Schimel et al., 1985; Scholten et al., 2017; Weintraub et al., 2015). However, there is little information on how terrain regulates the accumulation and distribution of SOC and its fractions (related to SOC stability) via biotic and abiotic factors in hilly regions. Such information would help to estimate forest SOC stocks and their dynamics.

Geostatistical methods are widely applied to the investigation of spatial variability in SOC (Dai et al., 2018; Hamzehpour et al., 2019; Liu et al., 2011). Semi-variograms and ordinary kriging are two of the most frequently used geostatistical methods (Yang et al., 2016; Yao et al., 2019). At large scales, the total C stocks are influenced by climatic factors (Gruba and Socha, 2019; Wang et al., 2019). Generally, C stocks increase with increasing precipitation and decreasing temperature (Gruba and Socha, 2019; Wang et al., 2019). At regional and small scales, soil texture, temperature, pH, precipitation, topography, as well as the quantity and quality of plant residues (Cao et al., 2019), have been identified as potentially important influences on SOC distributions (Bai and Zhou, 2020; Hamzehpour et al., 2019; Schimel et al., 1985; Zhang et al., 2020). In hilly regions, the soil nutrient profiles changes systematically down the slopes. Kleiss (1970) found that the SOC along a hillside increased downslope. Lower slope positions and depressions typically have higher levels of SOC than slopes or ridgetops (Schimel et al., 1985), although this pattern may be reversed in sandhill terrain (Barnes and Harrison, 1982) and in areas affected by wind erosion. It is difficult to determine the causes of C accumulation in soils, since it may have been moved downslope or fixed in situ (Schimel et al., 1985). The convexity of landform units (concave and convex shape) is a significant component of the terrain surface. At small scales, convexity can affect the distributions of water and nutrients, which may be important influences on SOC distributions.

Due to the complex terrain and high plant species richness of tropical forest ecosystems, spatial variations in SOC and its stability mechanism would be more complex and still need to be explored at the small scale. In this study, a large census data set from the 60 ha tropical montane rainforest dynamic monitoring plot at Hainan Island, China (Xu et al., 2015a), provides an ideal setting for studying the spatial distribution of SOC and the mechanisms of SOC stability. Soil samples at depths of 0–10 cm were collected from 60 subplots (20 m \times 20 m) randomly distributed in the plot. SOC and its physical and chemical fractions, other soil properties, plant species, root biomass and soil microorganisms were also measured. The aim of this study was to examine whether the spatial patterns in SOC and SOC stability mechanisms in an old-growth tropical rainforest are influenced by terrain, and to examine whether the influence of abiotic on SOC is more important for than biotic. The results provide basic information for understanding SOC distributions and stability mechanisms, and for modeling SOC spatiotemporal dynamics in tropical forests.

2. Materials and methods

2.1. Study area

This study was conducted in the Jianfengling National Nature Reserve (18°23'–18°50' N, 108°36'–109°05' E; altitude range: 0–1412 m), which is located in the southwestern region of Hainan Island, South China (Xu et al., 2015a). The region has a tropical monsoon climate with distinct wet and dry seasons (Yang et al., 2018), mean annual precipitation of 1300–3700 mm (most falling in May–October), and a mean annual temperature of 24.5 °C (Xu et al., 2015b). The main plant families in the study area are Lauraceae, Rubiaceae, Fagaceae, and Myrtaceae (Xu et al., 2015b). The region has an irregular topography with the predominant soil parent material being granite (Yang et al., 2018). The soil is yellow soil belonging to the Acrisols, according to the World Reference Base for Soil Resources.

2.2. Soil sampling and analyses

Based on the survey technical specifications of the Center for Tropical Forest Science, Smithsonian Institute (<http://www.ctfs.si.edu/doc/index.php>), the 60 ha tropical montane rainforest dynamic monitoring plot was divided into 1500 subplots, each 20 m \times 20 m in size. There were no large rivers or lakes, and the vegetation had a continuous distribution throughout the 60 ha tropical montane rainforest dynamic monitoring plot. The plot had certain topographical fluctuations that provided a variety of habitats suitable for studying the relationships between plants and habitats. The community and topography characteristics of each subplots were investigated in 2012 (Xu et al., 2015b). The altitude, latitude and longitude of the four corners and center of the 1500 subplots were recorded using a global positioning system (GPS). The average altitude of each subplot was taken as the average of the altitudes at the four corners, while the convexity of the subplot was the average altitude of the subplot minus the average altitude of the eight adjacent subplots. For the subplots located on the edges of the 60-ha plot, the convexity was taken as the altitude of the center of the subplot minus the average altitude of the four vertices of the 60-ha plot (Debski et al., 2002; Xu et al., 2015b). Cluster analysis of the 60-ha plot's terrain data found that the southwestern corner of the 60-ha plot had relatively gentle slopes, with the overall terrain gradually rising in elevation towards the northeast and becoming a steep ridge in the northeastern corner. The terrain was roughly divided into four types: flat land, gentle slopes, mid-slopes, and ridges (Xu et al., 2015b). In each terrain type, 15 subplots were randomly selected, making a total 60 subplots used in this study (Fig. 1).

Root samples were collected at each subplot at depths of 0–10 cm and 10–20 cm using an auger (10 cm diameter). The root samples were cleaned of residual soil particles with deionized water and divided into the first to fifth order roots. Each root order was spread out on a water-filled, transparent plastic tray and scanned with a graphic scanner (Expression 10000XL 1.0, Epson Telford Ltd., Telford, UK; dpi = 600). The resulting scans were analyzed by WinRHIZO software (Regent Instruments, Canada) to determine the average root diameter according to the methodology described by Metcalfe et al. (2008). Then, roots with diameters of ≤ 2 mm were defined as fine roots (Jackson et al., 1997), and were oven-dried at 65 °C until a constant weight was achieved (to the nearest = 0.0001 g).

One month before the root respiration measurement, the PVC collars (inner diameter = 20 cm, height = 15 cm) were inserted in each 20 m \times 20 m sample plot according to Fig. 1. And those PVC collars were inserted in the soil at a depth of 10 cm for measuring the total soil respiration. Meanwhile, the other PVC collars (inner diameter = 20 cm, height = 85 cm) were inserted in the soil at a depth of 80 cm at each subplot for measuring soil respiration (non-root respiration) without root respiration. Then, the total soil respiration minus the non-root respiration was taken as an estimate of the root respiration.

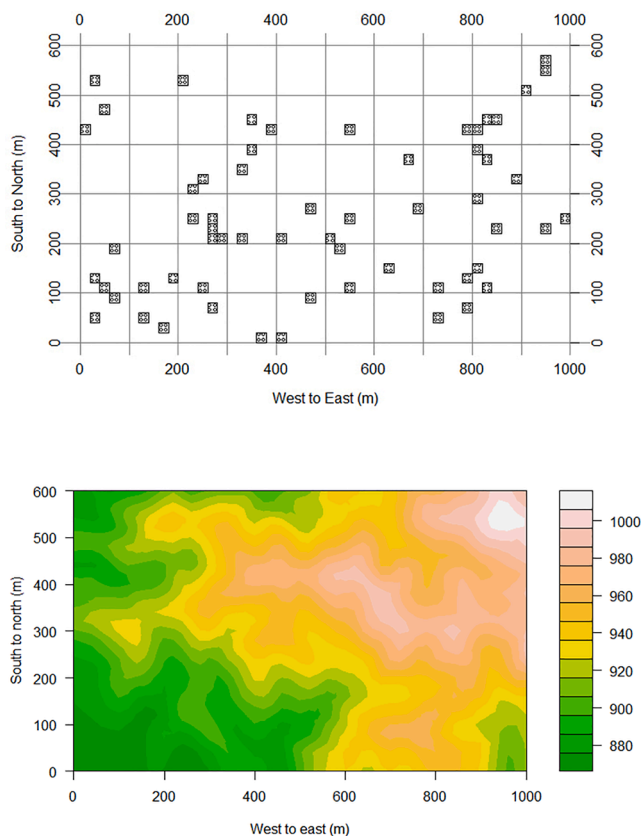


Fig. 1. Locations of the 60 subplots (top) and the topography (bottom; altitude, m) of the 60-ha tropical montane rainforest dynamics monitoring plot at Jianfengling, Hainan Island.

We collected four samples from topsoil (0–10 cm) in each subplot using an auger (5 cm diameter), with the distances between the four samples being <8 m. In total, 240 soil samples from the 60 subplots were collected and shipped to a laboratory within 24 h. The samples were divided into two parts: one part was stored at 4 °C to measure microbial biomass C (MBC), dissolved organic C (DOC), soil $\text{NH}_4^+\text{-N}$, $\text{NO}_3^-\text{-N}$, and soil enzyme activity. The other portions were air-dried and sieved to 2 mm to measure the physical fractions of SOC (including light fraction C, LFC; HFC), chemical fractions of SOC (i.e. alkyl C, O-alkyl C, aromatic C, carboxyl C), total nitrogen (TN), total phosphorous (TP), available phosphorous (AP) and soil pH values.

The SOC was detected using the modified Walkley–Black method (Lettenns et al., 2005). To determine MBC, 20 g fresh soil (<2 mm) was fumigated and extracted by CHCl_3 and $0.5 \text{ mol L}^{-1} \text{ K}_2\text{SO}_4$, with k_{EC} set to 0.45 (Wu et al., 1990). The DOC was measured following the method described by Jones and Willett (2006). LFC was determined using the density fractionation method, while HFC was calculated as the difference between SOC and LFC.

To determine SOC chemical fractions, soil samples were analyzed with ^{13}C CPMAS/NMR after being pretreated with 10% (v/v) HF solution (Mathers et al., 2002). The CPTOSS ^{13}C resonant frequency and ^1H resonant frequency was set to 100.38 MHz and 399.16 MHz, respectively. The rotate speed was set to 5 kHz, while the contact time was 3 ms with a cycle time is 1s, and data points was 4000. According to Baldock et al (1992), peaks at 0–45 ppm, 45–110 ppm, 110–160 ppm, and 160–220 ppm indicate the contents of alkyl C, O-alkyl C, aromatic C and carbonyl C, respectively. The measurements were conducted at the Analytical Center of the Institute of Chemistry, Chinese Academy of Sciences (Beijing).

Soil $\text{NH}_4^+\text{-N}$ and $\text{NO}_3^-\text{-N}$ contents were extracted using 2 M KCl, and the extracts were analyzed by a continuous flow analytical system

(SKALAR San++, SKALAR Co., Netherlands). Soil urease activity was determined by spectrophotometry at 578 nm in terms of the $\text{NH}_4^+\text{-N}$ released from 1.0 g of soil after 24 h incubation at 37 °C with 10% (w/v) urea solution in 20 mL of 1 M citrate buffer at pH 6.7 (Kandeler and Gerber, 1988). Soil catalase activity was measured as back-titration residual H_2O_2 was added to soil with 0.1 M KMnO_4 , and acid phosphatase activity was determined by the phosphoric acid bisacid colorimetric method (Guan, 1986).

2.3. Statistical analyses

In this study, geostatistical analysis was applied to determine the spatial patterns in SOC and its fractions. In detail, the degree of spatial continuity in soil properties and their range of spatial dependency, calculated as semi-variograms, were constructed with GS^+ software. To calculate semivariograms for a given separation distance h , data that were not normally distributed were logarithmically transformed (Liu et al., 2011), and then calculated according to the following formula:

$$\gamma(h) = \frac{1}{2N(h)} \sum_{i=1}^{2N(h)} [Z(x_i) - Z(x_i + h)]^2 \quad (1)$$

where $\gamma(h)$ is the semi-variance for a given separation distance h ; $Z(x_i)$ is the value of the variable Z at location x_i , and $N(h)$ is the number of pairs of sample points separated by the lag distance h . The best-fit models of SOC and its fractions were those with the largest coefficient of determination (R^2) and the smallest residuals (Yao et al., 2019). These models were selected to generate spatially continuous distribution maps of SOC and its fractions.

Random variation, caused mainly by measurement error or variations that could not be detected at the minimum sampling distance, was represented as the nugget effect (A_0). The sill, a constant value ($A + A_0$), commonly results from semivariance that increases with sampling distance (Trangmar et al., 1986). The range of spatial dependence equals the separation distance at which the sill is achieved (Webster and Oliver, 2007). The distances between samples that were lower than this range were spatially related, while those with greater distances were not spatially related. We classified the spatial dependence of soil properties according to the structure ratios of $A/(A + A_0)$. Variables with ratios >0.75 were considered to have strong spatial dependence; ratios of 0.25–0.75 indicate moderate dependence; and ratios <0.25 represent variables with weak dependence (Zhang et al., 2014).

To distinguish the main factors controlling the spatial distribution of SOC in different terrain among the 60 subplots, multiple regression tree analysis (MRT) was performed. The 60 subplots were classified into different terrain types by MRT according to the SOC and its physical components. The dependent variables of the MRT were SOC, DOC, LFC, and MBC, while the independent variables were altitude, convexity, and slope for each subplot. Similarly, MRT was used to analyze the chemical fractions of SOC. The dependent variables of the MRT were the fractions of alkyl C, O-alkyl C, aromatic C, carboxyl C, while the independent variables were altitude, convexity, and slope. Redundant analysis (RDA) was used to explain the variations in SOC and its fractions according to biotic and abiotic variables. The biotic variables included the number of all plant species, number of legume species, average height of all plants, average height of legume species, average basal area of all species, average basal area of legumes, total biomass, biomass of legumes, and the fine root biomasses at 0–10 cm and 10–20 cm. The abiotic variables included total nitrogen, $\text{NH}_4^+\text{-N}$, $\text{NO}_3^-\text{-N}$, microbial biomass nitrogen, total phosphorus, available phosphorus, total potassium, available potassium, soil moisture, soil pH, soil catalase, urease, and acid phosphatase, and so on. Variables with higher interpretation rates were considered more important.

For geostatistical analysis, RDA and MRT, subplot averaged soil property data were used for all 60 subplots. Data on altitude, slope, convexity, the species of each free-standing stem with a diameter at

breast height of ≥ 1.0 cm (species nomenclature followed the Flora of China), original legume density, total biomass, and legume biomass for each subplot were obtained from our previous studies (Xu et al., 2015a, b).

RDA and correlation diagrams were constructed using CANOCO 4.5 software. The significant level was set at $\alpha = 0.05$. The analyses of MRT and spatial distribution were all performed in R 4.0.2 (software R Core Team, 2019).

3. Results

3.1. SOC and its fractions

The average SOC was 34.4 g kg^{-1} and the average HFC was 26.4 g kg^{-1} , which accounted for 76.9% of the SOC (Table 1). The average MBC was 0.2 g kg^{-1} and its coefficient of variation (53%) was the largest among the total 10 variables. Alkyl C accounted for 41.7% of the total of the SOC chemical fractions. The proportions of O-alkyl C, carboxyl C, and aromatic C were 33.1%, 22.9%, and 2.6%, respectively. The mean ratio of alkyl C/O-alkyl C was 1.3.

3.2. Spatial characteristics of SOC and its fractions

The semi-variograms indicate that the theoretical model of each indicator was the best fitting model (Figs. S1 and S2). The structure ratios of the spatial variation analyses of SOC, LFC, HFC, and MBC ranged from 0.56 to 0.71 (Table 2), indicating moderate spatial dependence. The structure ratio of the spatial variation analysis for DOC was 0.23, indicating weak spatial dependence. Ordinary kriging interpolation and the spatial distribution of contours exhibited similar spatial distributions of SOC, LFC, and HFC, which increased along the ridgeline and had patch-and band-shaped distributions (Fig. 2). The spatial distributions of the environmental factors related to SOC and its physical fractions are shown in Fig. S3. The distribution of convexity was highly similar to those of SOC and LFC.

The structure ratios for aromatic C, carboxyl C, and alkyl C/O-alkyl C ratios ranged from 0.44 to 0.63, which indicates moderate spatial dependence. The structure ratios for soil alkyl C and O-alkyl C ranged from 0.76 to 0.99, which indicates strong spatial dependence. The distributions of alkyl C and aromatic C were band-shaped with patches (Fig. 3). However, the distributions of soil carboxyl C and O-alkyl C were mainly band-shaped. High percentages of soil alkyl C and O-alkyl C were distributed along the ridgeline. The distribution of the SOC chemical stability index (ratios of alkyl C/O-alkyl C) showed a certain continuity with a band-shape (Fig. 3). Referring to the topographic map of the study area (Fig. 1), we found that high ratios of alkyl C/O-alkyl C were mainly distributed on hillsides and in valleys. The spatial distributions of the environmental factors related to the chemical fraction of SOC are shown in Fig. S4. The distributions of convexity and biomass were highly

Table 1

Characteristics of soil organic carbon (SOC) at depths of 0–10 cm in the tropical montane rainforests of Jianfengling ($n = 60$).

Item	Mean	Minimum	Maximum	SD	CV (%)
SOC (g kg^{-1})	34.4	16.1	69.6	9.5	28
DOC (g kg^{-1})	0.4	0.1	1.0	0.2	498
MBC (g kg^{-1})	0.2	0.1	0.5	0.1	538
LFC (g kg^{-1})	7.9	1.3	30.5	3.8	48
HFC (g kg^{-1})	26.4	4.3	54.3	7.3	28
Alkyl carbon (%)	41.7	31.7	52.0	4.0	10
O-alkyl carbon (%)	33.1	21.8	41.5	4.5	14
Aromatic carbon (%)	2.6	1.1	6.9	1.1	43
Carboxyl carbon (%)	22.9	18.7	28.0	2.5	11
Ratios of alkyl carbon / O-alkyl carbon	1.3	0.8	2.0	0.3	21

SD: standard deviation; CV: coefficient of variation.

similar to that of alkyl C; the distributions of soil moisture, altitude, and soil urease were highly similar to that of O-alkyl C; the distribution of the basal area of legumes was highly similar to that of aromatic C; and the distributions of convexity and legume species were highly similar to that of carboxyl C (Fig. S4).

After 1000-fold cross-validation of MRT, altitude, and convexity were selected as independent variables and the MRTs of the 60 subplots were divided into three terrain types (type 1, 2, and 3) according to the SOC and its physical fractions (Fig. 4). Terrain types 1 and 2 were located in low-altitude (< 885 m, convexity < 0.8) and high-altitude valley areas (≥ 885 m, convexity < 0.8), while terrain type 3 occupied ridge areas (≥ 885 m, convexity ≥ 0.8). Convexity and pH were the important regulators of SOC and its physical fractions in terrain type 1. $\text{NH}_4^+\text{-N}$, TP, and TN were the important regulators of SOC and its physical fractions in terrain type 2. The pH, $\text{NO}_3^-\text{-N}$, $\text{NH}_4^+\text{-N}$, and TP were the important regulators of SOC and its physical fractions in terrain type 3 (Fig. 5).

The RDA results revealed that convexity, TN, altitude, pH, TP, $\text{NO}_3^-\text{-N}$, fine root biomass (0–10 cm), $\text{NH}_4^+\text{-N}$ (0–10 cm) and total root respiration explained 38.2%, 9.5%, 4.1%, 3.4%, 3.0%, 2.9%, 2.6%, 2.2%, and 1.9% of the variation in SOC and its physical fractions, respectively (Fig. 5). The RDA model revealed that the combined effect of the first two axes explained 96.1% of the total variance, while the first axis alone accounted for 88.4% (Table S1).

Using the abiotic factors as covariates, partial RDA showed that biotic factors accounted for 17.0% of the variation in SOC and its physical fractions, while the only statistically significant biotic factors, fine root biomass, could only explain 4.4% (Table S2). SOC and its physical fractions were positively related to fine root biomass at depths of 0–10 cm in terrain types 1 and 2, but this relationship was negative in terrain type 3 (Fig. 6a). With biotic factors as covariates, partial RDA showed that the selected (statistically significant) abiotic factors accounted for 32.9% of the variation in SOC and its physical fractions (Table S2), while convexity, soil catalase, and TP only explained 21.9%, 7.0%, and 4.0%, respectively. SOC and its physical fractions were positively related to convexity and soil catalase in terrain type 1 and soil catalase in terrain type 2, and were negatively related to soil catalase in terrain type 3 (Fig. 6b).

After 1000-fold cross-validation by MRT, altitude, and convexity were selected as independent variables and the MRTs of the 60 subplots were divided into three terrain types according to the chemical fractions of SOC. Terrain types 1 and 2 were located in low-altitude (< 961 m, convexity < 2.9) and high-altitude areas (≥ 961 m, convexity < 2.9), respectively, while terrain type 3 occupied ridge areas (≥ 961 m, convexity ≥ 2.9 ; Fig. 7). The important regulators of the chemical fractions of SOC were, for terrain type 1, fine root biomass at depths of 0–10 cm, convexity, TN, and soil catalase, while for terrain type 2 they were convexity and soil catalase, and for terrain type 3 they were fine root biomass at depths of 0–10 cm and TN (Fig. 8).

The RDA model revealed that TN, convexity, TP, legume density, altitude, $\text{NH}_4^+\text{-N}$, fine root biomass at 0–10 cm, soil moisture, soil catalase, fine root biomass at 10–20 cm and root respiration explain 27.6%, 14.1%, 9.4%, 4.4%, 3.6%, 3.2%, 2.9%, 2.4%, 2.3%, 2.0% and 1.7% of the variation in the chemical fractions of SOC, respectively (Fig. 8). The combined effect of the first two axes explains 94.9% of the variation and the first axis alone accounts for 77.3% (Table S3).

With abiotic factors as covariates, partial RDA showed that the biotic factors accounted for 16.3% of the variation in the SOC chemical fractions, while the statistically significant biotic factors could only explain 5.7% (Table S4 and Fig. 9a). Fine root biomasses at depths of 0–10 cm and 10–20 cm could explain 3.8% and 1.9% of the variation in SOC chemical fractions respectively. With biotic factors as covariates, partial RDA showed that the abiotic factors accounted for 40.2% of the variation in SOC chemical fractions, while the statistically significant abiotic factors could only explain 36.5% (Table S4 and Fig. 9b). In fact, TN, convexity, TP, altitude, soil moisture and $\text{NH}_4^+\text{-N}$ could explain 16.0%,

Table 2
Semi-variant function models and parameters of SOC and its fractions in the tropical montane rainforests of Jianfengling.

Item	Model	Nugget (A_0)	Sill ($A_0 + A$)	Structure ratio $A/(A_0 + A)$	Range (m)	Coefficient (R^2)	RMSE
SOC	Spherical	0.006	0.014	0.71	166.6	0.96	7.115
LFC	Spherical	0.091	0.114	0.56	166.6	0.867	3.199
HFC	Exponent	0.831	1.093	0.57	62.41	0.957	5.643
DOC	Spherical	0.062	0.018	0.23	166.6	0.862	0.144
MBC	Gaussian	25.14	53.90	0.68	342.6	0.883	89.35
Alkyl carbon	Spherical	0.001	0.017	0.99	166.6	0.939	3.753
O-alkyl carbon	Exponent	0.084	0.264	0.76	166.6	0.952	2.601
Aromatic carbon	Spherical	0.205	0.159	0.44	131.7	0.952	5.538
Carboxyl carbon	Spherical	0.027	0.046	0.63	189.5	0.955	1.685
Ratio of alkyl/o-alkyl carbon	Exponent	0.027	0.038	0.59	166.6	0.944	0.325

RMSE: Root mean square error.

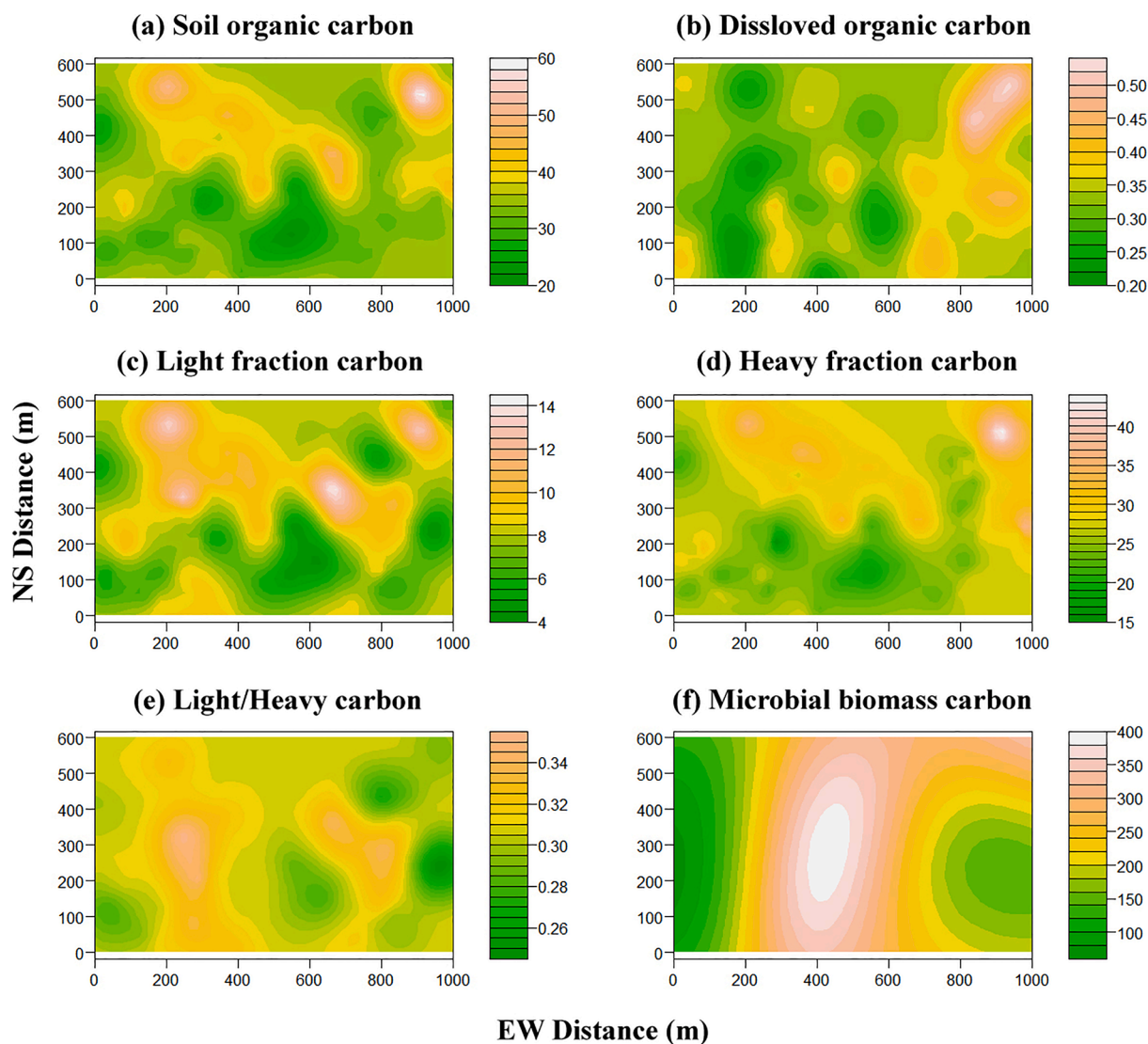


Fig. 2. Spatial distributions of soil organic carbon (a), dissolved organic carbon (b), light fraction carbon (c), heavy fraction carbon (d), ratio of light fraction carbon to heavy fraction carbon (e), and microbial biomass carbon (f) in the tropical montane rainforest of Jianfengling.

6.8%, 5.8%, 3.6%, 2.2%, and 2.1% of the variation in the SOC chemical fractions, respectively.

4. Discussion

4.1. Distribution of SOC physical and chemical stability and influencing factors

The spatial variations in SOC, HFC, and the chemical stability index of SOC (alkyl C/O-alkyl C) exhibited moderate spatial dependences,

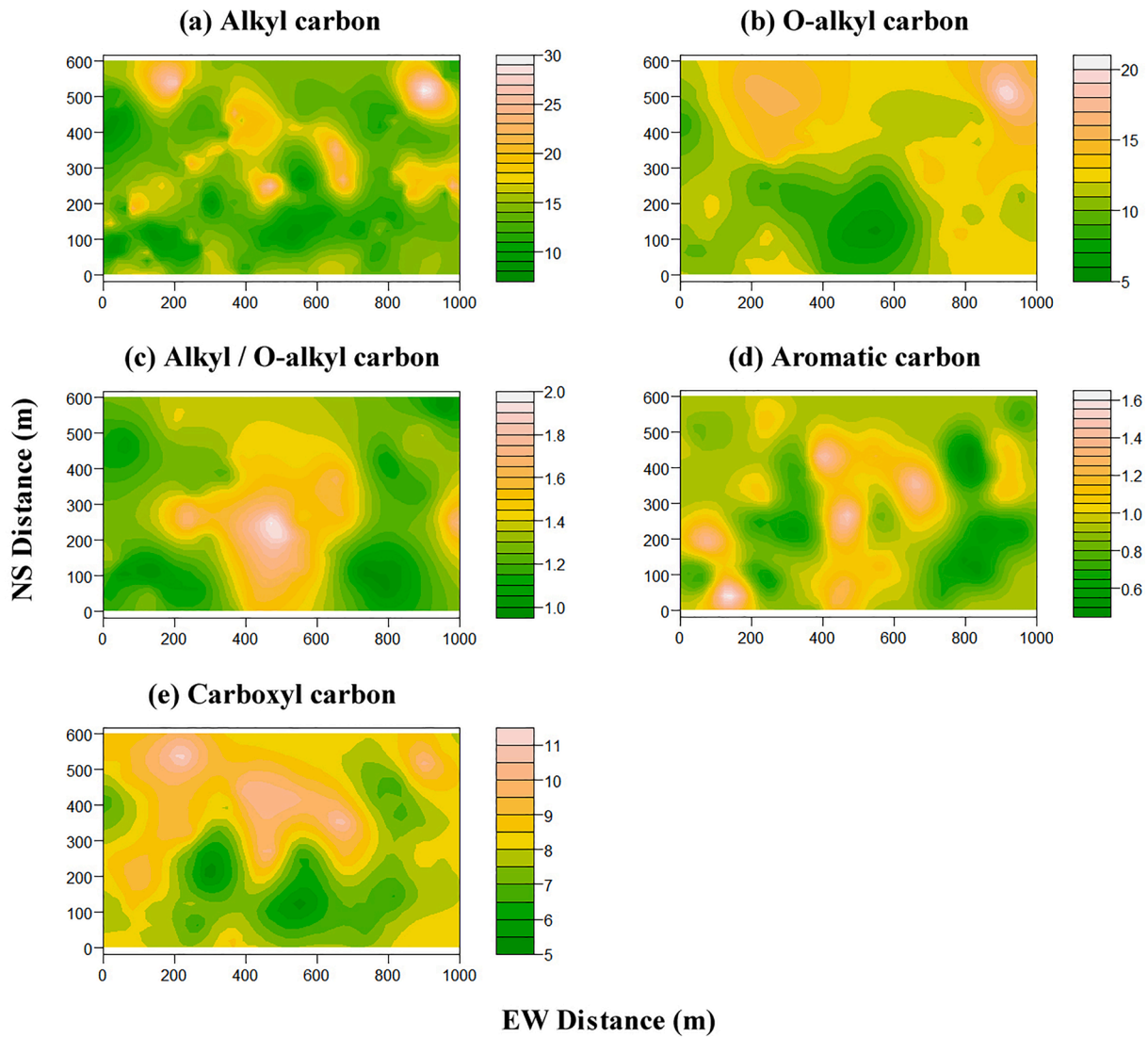


Fig. 3. Spatial distribution of the chemical fractions of soil organic carbon in the tropical montane rainforests of Jianfengling: (a) alkyl carbon; (b) O-alkyl carbon; (c) alkyl carbon/O-alkyl carbon; (d) aromatic carbon; and (e) carboxyl carbon.

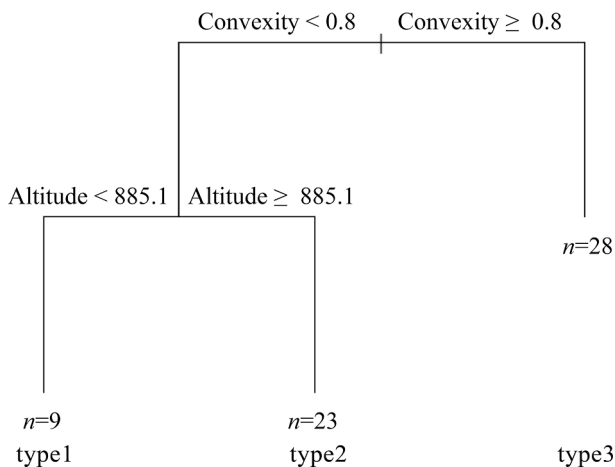


Fig. 4. Multivariate regression trees for 60 subplots of 20 m × 20 m in terms of SOC and its physical fractions in the tropical montane rainforests of Jianfengling (error: 0.642; CV error: 0.794; SE: 0.126).

indicating that there was a moderate heterogeneity in SOC and its fractions in the study area. The spatial variation in SOC is consistent with the findings of Guo et al. (2015), who used different sampling methods and data in the tropical montane rainforest of Jianfengling. However, our findings differ from a study conducted in a monsoon evergreen broad-leaf forest with relatively flat terrain in Dinghushan (Zhang et al., 2014) in terms of the spatial characteristics of SOC (high spatial autocorrelation and structure ratio of 0.936). Generally, the spatial dependences of places with strong man-made influences or relatively flat and uniform terrain are strong (Liu et al., 2011). The two research areas mentioned above are both in nature reserves and are relatively unaffected by human activity. Hence, it can be inferred that the complex topography of the study area caused the moderate heterogeneity in SOC and its fractions in the tropical montane rainforests of Jianfengling.

The distributions of SOC and HFC showed a certain continuity and a patch-shaped and band-shaped distribution (Fig. 2). We found that high SOC and high HFC were mainly distributed in the ridgeline and north-eastern areas of the plot, while low SOC appeared on hillsides and in valleys (Figs. 1 and 2). The results are consistent with previous studies conducted in a lowland evergreen broad-leaf rainforest in southern Taiwan (Tsui et al., 2004) and in a humid lowland tropical forest in

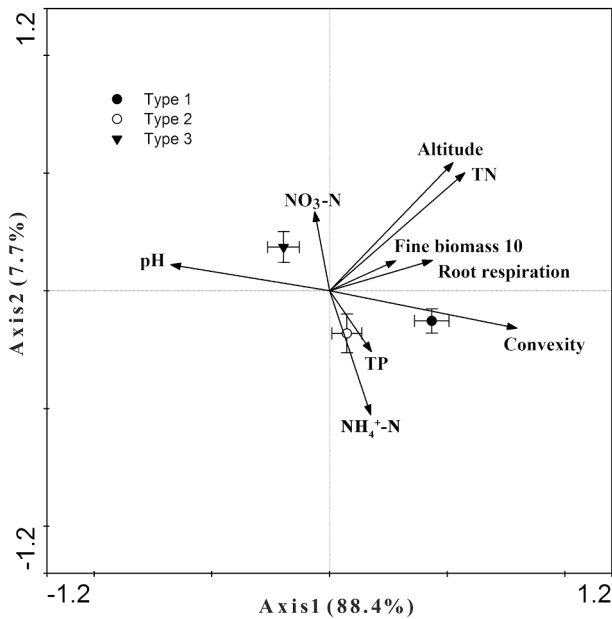


Fig. 5. The results of RDA between SOC and its physical fractions (light fraction C and heavy fractions C) and environment variables for different terrain types of subplots in the tropical montane rainforests of Jianfengling.

southwest Costa Rica (Weintraub et al., 2015), which found the highest SOC in ridgeline areas. Generally, steeper slopes contribute to greater runoff and greater translocation of surface materials downslope through surface erosion and movement of the soil mass (Hall, 1983). Carbon loss via soil erosion and decomposition results in SOC variations along a slope's gradient. Ridgeline areas with moderate gradients tend to have much higher SOC than other slope classes (Tsui et al., 2004). Convexity controls how water and soluble materials are distributed from higher to lower altitudes (Nizeyimana and Bicki, 1992). The accumulation of water and soluble materials on hillsides and in valleys could also be attributed to SOC and HFC decomposition, which usually results in low SOC and HFC accumulation. It indicates that terrain is an important influence on SOC distribution and stability at small scales in tropical montane rainforests. Terrain would also impact SOC decomposition and

transportation in different soil layers and so should be considered in future soil C cycle models (e.g. TECO and DELAC). In addition, valleys and ridges have different soil depths. Sufficient soil depth data from field investigations are required to model the relationships between terrain and soil depth.

The ratio of alkyl C/O-alkyl C reflects the degree of alkylation of SOC and has been used as an index of the degree of SOC decomposition or humification (Zhao et al., 2012). A higher ratio indicates a higher SOC decomposition degree (Webster et al., 2001). The distribution of the SOC chemical stability index (alkyl C/O-alkyl C) showed a certain continuity and a patch shape (Fig. 3). Unlike the physical fractions, the high ratios of alkyl C/O-alkyl C were mainly distributed on hillsides and in valleys. This result suggests that the high degree of SOC decomposition on hillsides and in valleys resulted in low SOC (Fig. 2). Potential explanations for this high alkyl C/O-alkyl C ratio include: 1) hillsides and valleys have relatively high temperatures that could promote microbial activity and SOC decomposition; and 2) higher nitrogen and water contents were found on hillsides and in valleys, which promote microbial activity and SOC decomposition. Meanwhile, TN (27.6%) and convexity (14.1%)

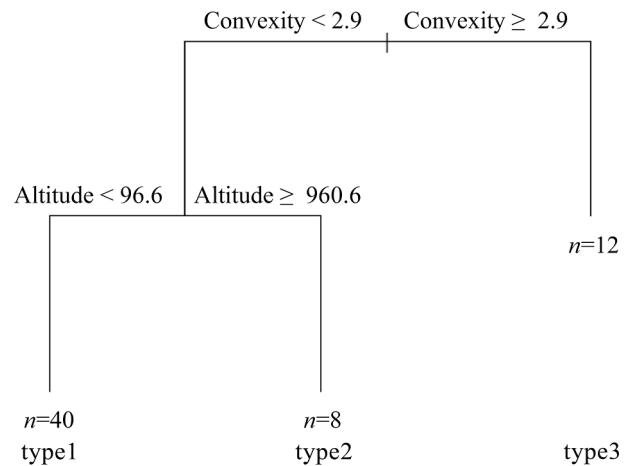


Fig. 7. Multivariate regression trees for 60 subplots of 20 m × 20 m according to the chemical fractions of SOC in the tropical montane rainforests of Jianfengling (error: 0.467; CV error: 0.883; SE: 0.175).

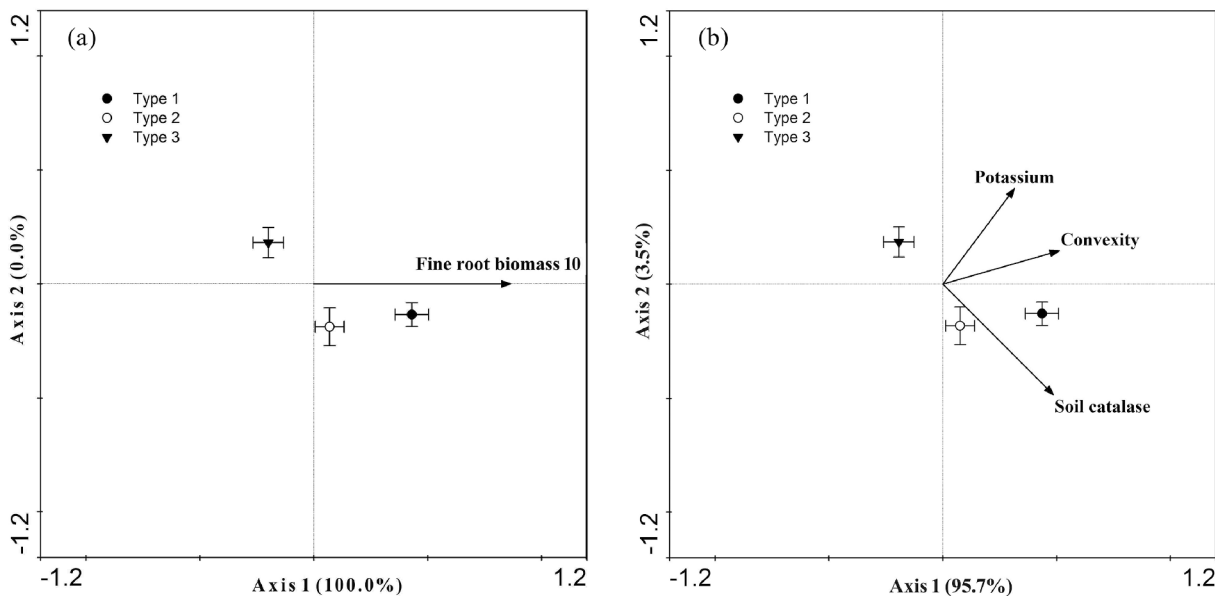


Fig. 6. Partial RDA diagrams of biotic (a) and abiotic environment variables (b) in relation to SOC and its physical fractions in the tropical montane rainforests of Jianfengling.

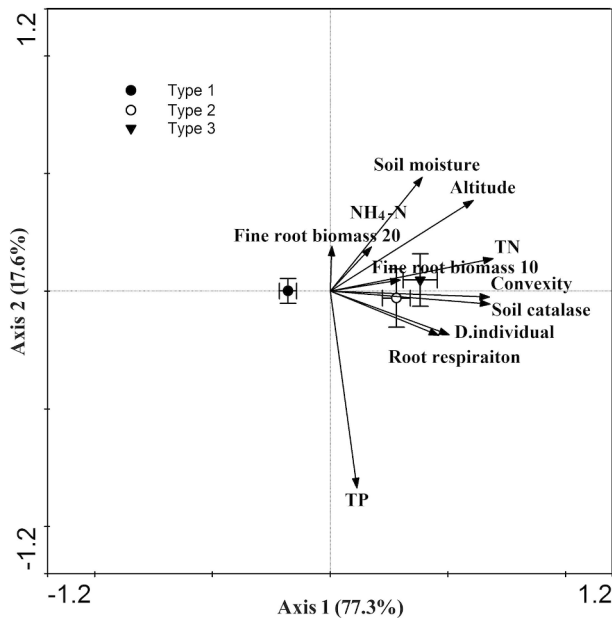


Fig. 8. RDA between chemical fractions of SOC and biotic and abiotic environmental factors in the tropical montane rainforests of Jianfengling.

best explained the spatial variations in SOC chemical fractions (Fig. 8).

4.2. Do biotic or abiotic factors control the distribution of SOC and its physical and chemical fractions?

Understanding the factors controlling SOC and its stability fractions is essential for C estimation, and is needed for management schemes that increase C sinks (Gruba and Socha, 2019). We found that the factors influencing the SOC (and its physical and chemical stability) distribution in the tropical rainforest were complex. Although convexity explained the spatial variations in SOC and its physical stability fractions the most, and TN and convexity best explained the spatial variations in the chemical fractions of SOC, the main influences on SOC and its fractions differed according to the type of terrain (Table S2). We next distinguished between the influences of biotic and abiotic factors on the distribution of SOC and its fractions.

Among biotic factors, fine root biomass at 0–10 cm was a significant

influence on the distribution of SOC and its physical and chemical fractions (Fig. 6a and 9a). Generally, C transported underground through below-ground net primary production is the main input for SOC (Gherardi and Sala, 2020). Fine roots are the below-ground plant organs with the highest production and turnover rates (Jackson et al., 1997; McCormack et al., 2015). In forest ecosystems, nutrients from the fine root biomass can return to the soil through litter decomposition and soil mineralization. Such processes partially determine the spatial variation in SOC and its fractions in rainforests (Finzi et al., 1998). In addition, root secretion and humus from root residues are also the main sources of SOC; hence, root distributions and detrital inputs of the root biomass contribute to SOC and its stability through rhizodeposition (Wilts et al., 2004). This is extremely important in regulating the accumulation and stability of SOC. In tropical rainforests, litter decomposition is rapid and roots can grow almost all year due to plentiful precipitation and warm temperatures. So, the influences of fine root on the accumulation and stability of SOC are significant.

Among the abiotic factors, convexity was an important influence on the distribution of SOC and its fractions (Fig. 6b and 9b). Convexity (which is related to aspect and slope) can control the movement of water and material down a slope, which contributes to spatial differences in soil properties at local scales (Buol et al., 2011). At the same time, the growth and distribution of vegetation in areas with different convexity are controlled by the bioavailability of soil nutrients (Kubota et al., 1998). Terrain gradients also control the local climate, vegetation distribution, and soil properties, as well as being associated with biogeochemical processes; e.g., SOC dynamics and its stability (Scholten et al., 2017). In addition, TN is another important influence on the distribution of SOC and its chemical fractions. Topography controls soil nitrogen availability in tropical forests (Weintraub et al., 2015), which may also influence vegetation and the microbial decomposition of litter (Finzi et al., 1998) and, therefore, the spatial variation in SOC and its chemical fractions.

The analyses of the physical and chemical fractions of SOC using RDA indicate that abiotic factors provided higher interpretation rates than biotic factors in all three terrain types, although abiotic and biotic factors had some covariance in this study. The related mechanism has been discussed above. This result highlights the influences of terrain on the distribution and accumulation of SOC in tropical rainforest ecosystems. Our results provide a reference for future studies on SOC and its stability, and on stability mechanisms in tropical rainforests with complex terrain and high plant species richness.

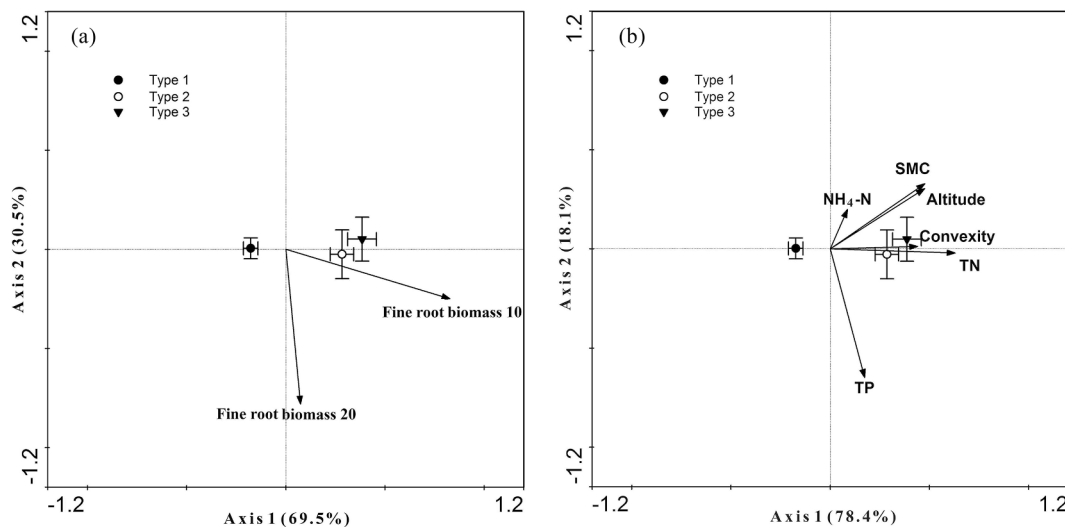


Fig. 9. Partial RDA diagram of biotic (a) and abiotic environment variables (b) in relation to soil chemical fractions carbon in the tropical montane rainforests of Jianfengling, respectively.

5. Conclusions

The spatial variations in the physical stability fractions of SOC and chemical stability index of SOC had moderate spatial autocorrelation in the Jianfengling Nature Reserve, due to its complex terrain. High SOC and its physical stability fractions were distributed along ridgelines, while high chemical stability indexes of SOC were mainly found on hillsides and in valleys. Convexity best explained the spatial variations in SOC and its physical stability fractions, while total nitrogen and convexity together best explained the spatial variations in the chemical fractions of SOC. In addition, this study indicates that abiotic factors have a greater influence on SOC and its fractions than biotic factors, while abiotic and biotic factors have some covariance. These findings provide a reference for subsequent classification research on tropical montane rainforests and highlight that terrain should be considered in C cycle models.

Funding

This work was supported by the National Natural Science Foundation of China [No. 41663010 and 41201061]; and the Scientific Research Foundation of Hainan University [No. kyqd1604 and kyqd1605]. The first author thanks for the financial support from China Scholarship Council.

CRediT authorship contribution statement

Wenjie Liu: Methodology, Writing - original draft. **Yamin Jiang:** Data curation, Software. **Qiu Yang:** Investigation, Validation. **Huai Yang:** Conceptualization, Project administration. **Yide Li:** Resources. **Zhaolei Li:** Conceptualization. **Wei Mao:** Software, Validation. **Yiqi Luo:** Writing - review & editing. **Xu Wang:** Supervision, Validation. **Zhenghong Tan:** Supervision.

Declaration of Competing Interest

The authors declare that they have no known competing financial interests or personal relationships that could have appeared to influence the work reported in this paper.

Acknowledgment

We are grateful to Jianfengling National Key Field Research Station for Tropical Forest Ecosystem for providing their assistance in field work.

Appendix A. Supplementary data

Supplementary data to this article can be found online at <https://doi.org/10.1016/j.ecolind.2021.107965>.

References

- Bai, Y.X., Zhou, Y.C., 2020. The main factors controlling spatial variability of soil organic carbon in a small karst watershed, Guizhou Province, China. *Geoderma* 357.
- Baldock, J.A., Oades, J.M., Waters, A.G., Peng, X., Vassallo, A.M., Wilson, M.A., 1992. Aspects of the chemical structure of soil organic materials as revealed by solid-state ^{13}C NMR spectroscopy. *Biogeochemistry* 16 (1), 1–42.
- Barnes, P.W., Harrison, A.T., 1982. Species distribution and community organization in a Nebraska Sandhills mixed prairie as influenced by plant/soil-water relationships. *Oecologia* 52 (2), 192–201.
- Buol, S.W., Southard, R.J., Graham, R.C., McDaniel, P.A., 2011. Soil-Forming Factors: Soil as a Component of Ecosystems. *Soil Genesis Classif.* 89–140.
- Cao, B.J., Domke, G.M., Russell, M.B., Walters, B.F., 2019. Spatial modeling of litter and soil carbon stocks on forest land in the conterminous United States. *Sci. Total Environ.* 654, 94–106.
- Ciais, P., Chris, S., Govindasamy, B., Bopp, L., Brovkin, V., Canadell, J., Chhabra, A., Defries, R., Galloway, J., Heimann, M., 2013. Carbon and other biogeochemical cycles. *Climate Change 2013: The Physical Science Basis*, 465–570.

- Cox, P.M., Betts, R.A., Jones, C.D., Spall, S.A., Totterdell, I.J., 2000. Acceleration of global warming due to carbon-cycle feedbacks in a coupled climate model. *Nature* 408 (6809), 184–187.
- Cramer, W., Bondeau, A., Woodward, F.I., Prentice, I.C., Betts, R.A., Brovkin, V., Cox, P.M., Fisher, V., Foley, J.A., Friend, A.D., Kucharik, C., Lomas, M.R., Ramankutty, N., Sitch, S., Smith, B., White, A., Young-Molling, C., 2001. Global response of terrestrial ecosystem structure and function to CO_2 and climate change: results from six dynamic global vegetation models. *Glob. Change Biol.* 7, 357–373.
- Dai, W., Li, Y., Fu, W., Jiang, P., Zhao, K., Li, Y., Penttinen, P., 2018. Spatial variability of soil nutrients in forest areas: A case study from subtropical China. *J. Plant Nutr. Soil Sci.* 181 (6), 827–835.
- Debski, I., Burslem, D.F.R.P., Palmiotto, P.A., Lafrankie, J.V., Lee, H.S., Manokaran, N., 2002. Habitat preferences of Aporosa in two Malaysian forests: implications for abundance and coexistence. *Ecology* 83 (7), 2005–2018.
- Finzi, A.C., Van Breemen, N., Canham, C.D., 1998. Canopy tree-soil interactions within temperate forests: species effects on soil carbon and nitrogen. *Ecol. Appl.* 8 (2), 440–446.
- Gherardi, L.A., Sala, O.E., 2020. Global patterns and climatic controls of belowground net carbon fixation. *P Natl Acad Sci USA* 117 (33), 20038–20043.
- Golchin, A., Clarke, P., Oades, J.M., Skjemstad, J.O., 1995. The effects of cultivation on the composition of organic-matter and structural stability of soils. *Soil Res.* 33 (6), 975. <https://doi.org/10.1071/SR9950975>.
- Gruba, P., Socha, J., 2019. Exploring the effects of dominant forest tree species, soil texture, altitude, and pH (H_2O) on soil carbon stocks using generalized additive models. *For. Ecol. Manage.* 447, 105–114.
- Guan, S.Y., 1986. *Soil Enzyme and Study Methods*. Agriculture Press, Beijing.
- Guo, X.W., Luo, T.S., Li, Y.D., Xu, H., Chen, D.X., Lin, M.X., Zhou, Z., Yang, H., 2015. Spatial distribution characteristics of soil organic carbon density in a tropical mountain rainforest of Jianfengling, Hainan Island, China. *Acta Ecologica Sinica* 35, 7878–7886.
- Hall, G.F., 1983. Chapter 5 – Pedology and Geomorphology. In: Wilding, L.P., Smeck, N.E., Hall, G.F. (Eds.), *Developments in Soil Science*. Elsevier, pp. 117–140.
- Hamzeshpour, N., Shafizadeh-Moghadam, H., Valavi, R., 2019. Exploring the driving forces and digital mapping of soil organic carbon using remote sensing and soil texture. *Catena* 182, 104141. <https://doi.org/10.1016/j.catena.2019.104141>.
- Jackson, R.B., Lajtha, K., Crow, S.E., Hugelius, G., Kramer, M.G., Piñeiro, G., 2017. The ecology of soil carbon: pools, vulnerabilities, and biotic and abiotic controls. *Annu. Rev. Ecol. Evol. Syst.* 48 (1), 419–445.
- Jackson, R.B., Mooney, H.A., Schulze, E.D., 1997. A global budget for fine root biomass, surface area, and nutrient contents. *Proc. Natl. Acad. Sci.* 94, 7362.
- Jones, D., Willett, V., 2006. Experimental evaluation of methods to quantify dissolved organic nitrogen (DON) and dissolved organic carbon (DOC) in soil. *Soil Biol. Biochem.* 38 (5), 991–999.
- Kandeler, E., Gerber, H., 1988. Short-term assay of soil urease activity using colorimetric determination of ammonium. *Biol. Fertil. Soils* 6, 68–72.
- Kleiss, H.J., 1970. Hillslope sedimentation and soil formation in Northeastern Iowa. *Soil Sci. Soc. Am. J.* 34 (2), 287–290.
- Kubota, D., Masunaga, T., Hermansah, Rasyidin, A., Hotta, M., Shinmura, Y., Wakatsuki, T., 1998. In: *Soils of Tropical Forest Ecosystems*. Springer Berlin Heidelberg, Berlin, Heidelberg, pp. 159–167. https://doi.org/10.1007/978-3-662-03649-5_18.
- Letten, S., Orshoven, J., Wesemael, B., Muys, B., Perrin, D., 2005. Soil organic carbon changes in landscape units of Belgium between 1960 and 2000 with reference to 1990. *Glob. Change Biol.* 11 (12), 2128–2140.
- Liu, W., Su, Y., Yang, R., Yang, Q., Fan, G., 2011. Temporal and spatial variability of soil organic matter and total nitrogen in a typical oasis cropland ecosystem in arid region of Northwest China. *Environ. Earth Sci.* 64 (8), 2247–2257.
- Luo, Y., Keenan, T.F., Smith, M., 2015. Predictability of the terrestrial carbon cycle. *Glob. Change Biol.* 21 (5), 1737–1751.
- Mathers, N.J., Xu, Z., Berners-Price, S.J., Perera, M.C.S., Saffigna, P.G., 2002. Hydrofluoric acid pre-treatment for improving ^{13}C CPMAS NMR spectral quality of forest soils in south-east Queensland, Australia. *Aust. J. Soil Res.* 40 (4), 655–674.
- McCormack, M.L., Dickie, I.A., Eissenstat, D.M., Fahey, T.J., Fernandez, C.W., Guo, D., Helmsaari, H.-S., Hobbie, E.A., Iversen, C.M., Jackson, R.B., Leppälammikujansuu, J., Norby, R.J., Phillips, R.P., Pregitzer, K.S., Pritchard, S.G., Rewald, B., Zadworny, M., 2015. Redefining fine roots improves understanding of below-ground contributions to terrestrial biosphere processes. *New Phytol.* 207 (3), 505–518.
- Merino, C., Nannipieri, P., Matus, F., 2014. Soil carbon controlled by plant, microorganism and mineralogy interactions. *J. Soil Sci. Plant Nutr.* 15 (2), 321–332.
- Metcalfe, D.B., Meir, P., Aragão, L.E.O.C., da Costa, A.C.L., Braga, A.P., Gonçalves, P.H.L., de Athaydes Silva Junior, J., de Almeida, S.S., Dawson, L.A., Malhi, Y., Williams, M., 2008. The effects of water availability on root growth and morphology in an Amazon rainforest. *Plant Soil* 311 (1–2), 189–199.
- Nizeyimana, E., Bicki, T.J., 1992. Soil and soil-landscape relationships in the north central region of Rwanda, east-central Africa. *Soil Sci.* 153 (3), 225–236.
- Pan, Y., Birdsey, R.A., Fang, J., Houghton, R., Kauppi, P.E., Kurz, W.A., Phillips, O.L., Shvidenko, A., Lewis, S.L., Canadell, J.G., Ciais, P., Jackson, R.B., Pacala, S.W., McGuire, A.D., Piao, S., Rautiainen, A., Sitch, S., Hayes, D., 2011. A large and persistent carbon sink in the world's forests. *Science* 333 (6045), 988–993.
- Schimel, D., Stillwell, M.A., Woodmansee, R.G., 1985. Biogeochemistry of C, N, and P in a soil catena of the shortgrass steppe. *Ecology* 66, 276–282.
- Scholten, T., Goebes, P., Kühn, P., Seitz, S., Assmann, T., Bauhus, J., Bruelheide, H., Buscot, F., Erfmeier, A., Fischer, M., Härdtle, W., He, J.-S., Ma, K., Niklaus, P.A., Scherer-Lorenzen, M., Schmid, B., Shi, X., Song, Z., von Oheimb, G., Wirth, C., Wubet, T., Schmidt, K., 2017. On the combined effect of soil fertility and topography

- on tree growth in subtropical forest ecosystems—a study from SE China. *J. Plant Ecol.*, 10, 111–127.
- Shi, Z., Crowell, S., Luo, Y., Moore, B., 2018. Model structures amplify uncertainty in predicted soil carbon responses to climate change. *Nat. Commun.* 9 (1) <https://doi.org/10.1038/s41467-018-04526-9>.
- Tao, F., Zhou, Z., Huang, Y., Li, Q., Lu, X., Ma, S., Huang, X., Liang, Y., Hugelius, G., Jiang, L., Doughty, R., Ren, Z., Luo, Y., 2020. Deep learning optimizes data-driven representation of soil organic carbon in earth system model over the conterminous United States. *Front. Big Data* 3. <https://doi.org/10.3389/fdata.2020.00017>.
- Trangmar, B.B., Yost, R.S., Uehara, G., 1986. Application of Geostatistics to Spatial Studies of Soil Properties. In: Brady, N.C. (Ed.), *Advances in Agronomy*. Academic Press, pp. 45–94.
- Trumbore, S.E., 1997. Potential responses of soil organic carbon to global environmental change. *Proc. Natl. Acad. Sci.* 94, 8284.
- Tsui, C.-C., Chen, Z.-S., Hsieh, C.-F., 2004. Relationships between soil properties and slope position in a lowland rain forest of southern Taiwan. *Geoderma* 123 (1-2), 131–142.
- von Lütow, M., Kögel-Knabner, I., Ekschmitt, K., Flessa, H., Guggenberger, G., Matzner, E., Marschner, B., 2007. SOM fractionation methods: relevance to functional pools and to stabilization mechanisms. *Soil Biol. Biochem.* 39 (9), 2183–2207.
- Wang, H., Liu, S.-R., Mo, J.-M., Wang, J.-X., Makeschin, F., Wolff, M., 2010. Soil organic carbon stock and chemical composition in four plantations of indigenous tree species in subtropical China. *Ecol. Res.* 25 (6), 1071–1079.
- Wang, S., Zhuang, Q., Yang, Z., Yu, N.a., Jin, X., 2019. Temporal and spatial changes of soil organic carbon stocks in the forest area of Northeastern China. *Forests* 10 (11), 1023. <https://doi.org/10.3390/f10111023>.
- Webster, E.A., Hopkins, D.W., Chudek, J.A., Haslam, S.F.I., Šimek, M., Píček, T., 2001. The relationship between microbial carbon and the resource quality of soil carbon. *J. Environ. Qual.* 30 (1), 147–150.
- Webster, R., Oliver, M., A., 2007. *Characterizing Spatial Processes: The Covariance and Variogram*. Geostatist. Environ. Sci., 47–76.
- Weintraub, S.R., Taylor, P.G., Porder, S., Cleveland, C.C., Asner, G.P., Townsend, A.R., 2015. Topographic controls on soil nitrogen availability in a lowland tropical forest. *Ecology* 96 (6), 1561–1574.
- Wilts, A.R., Reicosky, D.C., Allmaras, R.R., Clapp, C.E., 2004. Long-Term Corn Residue Effects: Harvest Alternatives, Soil Carbon Turnover, and Root-Derived Carbon. *Soil Sci. Soc. Am. J.* 68 (4), 1342–1351.
- Wu, J., Joergensen, R.G., Pommerening, B., Chaussod, R., Brookes, P.C., 1990. Measurement of soil microbial biomass C by fumigation-extraction—an automated procedure. *Soil Biol. Biochem.* 22 (8), 1167–1169.
- Xu, H., Detto, M., Fang, S., Li, Y., Zang, R., Liu, S., Nardoto, G.B., 2015a. Habitat hotspots of common and rare tropical species along climatic and edaphic gradients. *J. Ecol.* 103 (5), 1325–1333.
- Xu, H., Li, Y., Lin, M., Wu, J., Luo, T., Zhou, Z., Chen, D., Yang, H., Li, G., Liu, S., 2015b. Community characteristics of a 60 ha dynamics plot in the tropical montane rain forest in Jianfengling, Hainan Island. *Biodiversity Sci.* 23, 192–201.
- Yang, H., Liu, S., Li, Y., Xu, H., 2018. Diurnal variations and gap effects of soil CO₂, N₂O and CH₄ fluxes in a typical tropical montane rainforest in Hainan Island, China. *Ecol. Res.* 33 (2), 379–392.
- Yang, P., Byrne, J.M., Yang, M., 2016. Spatial variability of soil magnetic susceptibility, organic carbon and total nitrogen from farmland in northern China. *Catena* 145, 92–98.
- Yao, X., Yu, K., Deng, Y., Zeng, Q., Lai, Z., Liu, J., 2019. Spatial distribution of soil organic carbon stocks in Masson pine (*Pinus massoniana*) forests in subtropical China. *Catena* 178, 189–198.
- Yu, M., Wang, Y., Jiang, J., Wang, C., Zhou, G., Yan, J., 2019. Soil organic carbon stabilization in the three subtropical forests: importance of clay and metal oxides. *J. Geophys. Res.-Biogeosci.* 124 (10), 2976–2990.
- Zhang, H., Goll, D.S., Wang, Y., Ciais, P., Wieder, W.R., Abramoff, R., Huang, Y., Guenet, B., Prescher, A., Viscarra Rossel, R.A., Barré, P., Chenu, C., Zhou, G., Tang, X., 2020. Microbial dynamics and soil physicochemical properties explain large scale variations in soil organic carbon. *Glob. Change Biol.* 26 (4), 2668–2685.
- Zhang, Y., Ouyang, X., Chu, G., Zhang, Q., Liu, S., Zhang, D., Li, Y., 2014. Spatial heterogeneity of soil organic carbon and total nitrogen in a monsoon evergreen broadleaf forest in Dinghushan, Guangdong, China. *Ying Yong Sheng Tai Xue Bao* 25 (1), 19–23.
- Zhao, H., Lv, Y., Wang, X., Zhang, H., Yang, X., 2012. Tillage impacts on the fractions and compositions of soil organic carbon. *Geoderma* 189-190, 397–403.